

# Optimized Inhibitors of MDM2 via an Attempted Protein-Templated Reductive Amination

Ramon van der Vlag<sup>+, [a]</sup>, M. Yagiz Unver<sup>+, [a]</sup>, Tommaso Felicetti<sup>+, [a, b]</sup>, Aleksandra Twarda-Clapa,<sup>[c]</sup> Fatima Kassim,<sup>[a]</sup> Cagdas Ermis,<sup>[a]</sup> Constantinos G. Neochoritis,<sup>[d, e]</sup> Bogdan Musielak,<sup>[c]</sup> Beata Labuzek,<sup>[c]</sup> Alexander Dömling,<sup>[d]</sup> Tad A. Holak,<sup>[c]</sup> and Anna K. Hirsch<sup>\*[a, f, g]</sup>

Innovative and efficient hit-identification techniques are required to accelerate drug discovery. Protein-templated fragment ligations represent a promising strategy in early drug discovery, enabling the target to assemble and select its binders from a pool of building blocks. Development of new protein-templated reactions to access a larger structural diversity and expansion of the variety of targets to demonstrate the scope of the technique are of prime interest for medicinal chemists. Herein, we present our attempts to use a protein-templated reductive amination to target protein-protein

interactions (PPIs), a challenging class of drug targets. We address a flexible pocket, which is difficult to achieve by structure-based drug design. After careful analysis we did not find one of the possible products in the kinetic target-guided synthesis (KTGS) approach, however subsequent synthesis and biochemical evaluation of each library member demonstrated that all the obtained molecules inhibit MDM2. The most potent library member ( $K_i = 0.095 \mu\text{M}$ ) identified is almost as active as Nutlin-3, a potent inhibitor of the p53-MDM2 PPI.

[a] R. van der Vlag,<sup>+</sup> M. Yagiz Unver,<sup>+</sup> Dr. T. Felicetti,<sup>+</sup> F. Kassim, C. Ermis, Prof. Dr. A. K. H. Hirsch  
Stratingh Institute for Chemistry  
University of Groningen  
Nijenborgh 7  
9747 AG Groningen (The Netherlands)

[b] Dr. T. Felicetti<sup>+</sup>  
Department of Pharmaceutical Sciences  
University of Perugia  
Via del Liceo 1  
06123 Perugia (Italy)

[c] Dr. A. Twarda-Clapa, Dr. B. Musielak, B. Labuzek, Prof. Dr. T. A. Holak  
Faculty of Chemistry  
Jagiellonian University  
Gronostajowa 2  
30-387 Krakow (Poland)


[d] Dr. C. G. Neochoritis, Prof. Dr. A. Dömling  
Department of Pharmacy, Drug Design group  
University of Groningen  
A. Deusinglaan 1  
Groningen (The Netherlands)


[e] Dr. C. G. Neochoritis  
Chemistry department, University of Crete, 70013 Heraklion, Greece

[f] Prof. Dr. A. K. H. Hirsch  
Department of Drug Design and Optimization  
Helmholtz Institute for Pharmaceutical Research Saarland (HIPS) –  
Helmholtz Centre for Infection Research (HZI)  
Campus Building E8.1  
66123 Saarbrücken (Germany)  
E-mail: Anna.Hirsch@helmholtz-hips.de

[g] Prof. Dr. A. K. H. Hirsch  
Department of Pharmacy  
Saarland University  
Campus Building E8.1  
66123 Saarbrücken (Germany)

[†] These authors contributed equally to this work.

 Supporting information for this article is available on the WWW under <https://doi.org/10.1002/cmdc.201900574>

 © 2019 The Authors. Published by Wiley-VCH Verlag GmbH & Co. KGaA. This is an open access article under the terms of the Creative Commons Attribution Non-Commercial License, which permits use, distribution and reproduction in any medium, provided the original work is properly cited and is not used for commercial purposes.

## Introduction

Discovery of fast and efficient techniques to identify bioactive compounds constitutes an important part in today's drug discovery. A way to accelerate hit-identification is the use of reversible reactions (dynamic combinatorial chemistry, DCC) or irreversible reactions (kinetic target-guided synthesis, KTGS), which are both categories of templated fragment ligations.<sup>[1]</sup> In these templated fragment ligations, the target selects its own inhibitors by assembling the corresponding binders from a library of complementary building blocks or by binding and amplifying them from a library of compounds formed in a covalent bond-forming reaction. In KTGS, the biological target accelerates the irreversible reaction between complementary building blocks upon binding,<sup>[2,3]</sup> whereas in DCC a reversible reaction between building blocks affords a dynamic combinatorial library (DCL) from which the biological target selects and amplifies the best binder(s).<sup>[4,5]</sup> Both techniques hold the potential to accelerate drug discovery and are still relatively underexplored, especially in terms of target scope and availability of biocompatible reactions.

KTGS is a promising hit-identification strategy but only a few reactions with a limited number of targets have been reported so far.<sup>[1,2,6–19]</sup> The most widely used reaction is the Huisgen 1,3-dipolar cycloaddition of azides and alkynes and most work in KTGS focuses on acetylcholine esterase (AChE) from various species, although different reactions and targets have been explored.<sup>[2,3]</sup>

Protein-protein interactions (PPIs) are involved in many biological functions, such as intercellular communication and apoptosis. Targeting PPIs using small molecules is considered challenging given the flatness of the interface, a lack of small-

molecule starting points for the future design and the difficulties in distinguishing real from artefactual binding.<sup>[20]</sup>

p53 is a tumor-suppressor protein that is activated by cellular stress or damage and leads to cell-cycle arrest, apoptosis and DNA repair. MDM2 is the negative regulator of the p53 protein and its overexpression leads to loss of p53 function.<sup>[21,22]</sup> MDM2 has a well-defined and deep pocket, unusual for PPIs, accommodating a hotspot triad consisting of Trp23, Leu26 and Phe19 from p53.<sup>[21,23,24]</sup> Therefore, design of high-affinity ligands to inhibit MDM2 should focus on these hotspot amino acids of p53 (three-point pharmacophore model). As a result, several small-molecule inhibitors have been reported.<sup>[23–26]</sup> Some time ago, we found the Leu26 pocket to be a flexible pocket, which is enlarged upon ligand binding (four-point pharmacophore model).<sup>[27]</sup> Very recently, we expanded this work with a thorough SAR analysis.<sup>[28]</sup> The flexibility of the pocket makes it very difficult to target using structure-based drug design (SBDD) or other computational techniques such as virtual screening. Therefore, KTGS holds the potential to explore this flexible binding pocket by letting the protein select which combination of building blocks ideally fits.

Use of protein-templated reactions to interrupt PPIs has only been shown for the Bcl-XL/BAK interaction<sup>[11,17]</sup> and the 14-3-3 protein.<sup>[7]</sup> These targets feature deep cavities in the binding pocket, which makes them suitable for KTGS just like MDM2. The reactions used for these two targets are the sulfo-click reaction between thio acids and sulfonyl azides and  $S_N2$  thiol ring opening of epoxides, respectively.

The reversible reaction between an aldehyde and an amine to afford imines has been widely applied in DCC to target various biological targets (Figure 1).<sup>[29–39]</sup> It is generally believed that the assembly of inhibitors is achieved by simultaneous binding of both building blocks in adjacent pockets, followed by imine formation and subsequent reduction, resulting in an irreversible amine bond. However, since in most cases the reducing agent is present in the mixture during most of the reaction time, it is unknown if this is actually true and difficult, if not impossible, to prove. Additionally, we think that protein-templated reductive amination is an example of KTGS instead of genuine DCC, in which the formed bond remains non-covalent.

Since the formed imines are unstable in aqueous media, *in situ* reduction is performed in most cases. After analysis, frequently only the most amplified hits are synthesized and tested for activity. This approach, however, represents several pitfalls, such as: 1) it is assumed that the imines have a similar

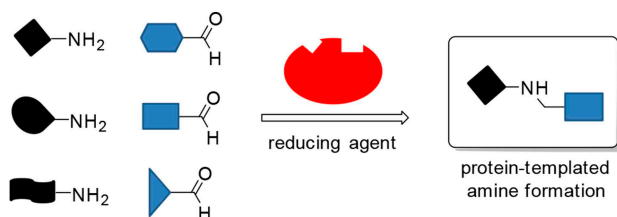


Figure 1. Protein-templated reductive amination.

binding mode as the amines; and 2) the potency of the compound might change upon reduction. Previously, large differences in potency between imine and amine have been reported.<sup>[31,39]</sup> Furthermore, we noticed that in most reports the potencies of the starting materials are not reported, although many of the starting materials are used as anchors.

Herein, we present our efforts to use protein-templated reductive amination in the KTGS context for the identification of inhibitors of the MDM2-p53 PPI. Additionally, it is the first application of KTGS to address a flexible binding pocket (Leu26 pocket). Given that we were unable to observe any of the reductive amination products, we evaluated all members of the library.

## Results and Discussion

After the discovery of the extended Leu26 pocket in MDM2,<sup>[27]</sup> we set out to explore this flexible pocket. Having selected MDM2 as a target, we designed our potential inhibitor scaffold starting from the X-ray crystal structure of inhibitor 1 in complex with MDM2 (Figure 2, PDB ID: 4MDN).<sup>[27]</sup>

We designed and optimized a new inhibitor by using the molecular modeling program SeeSAR.<sup>[40]</sup> Inhibitor 1 occupies the three sub-pockets of MDM2 that are named according to the corresponding p53 residues: the 6-chloroindole-2-hydroxamic acid moiety is hosted by the Trp23 pocket, the *tert*-butyl group occupies the Phe19 pocket and the large 4-chlorobenzyl phenyl ether was found to fill the Leu26 and an induced sub-pocket. In order to occupy this extended sub-pocket in an

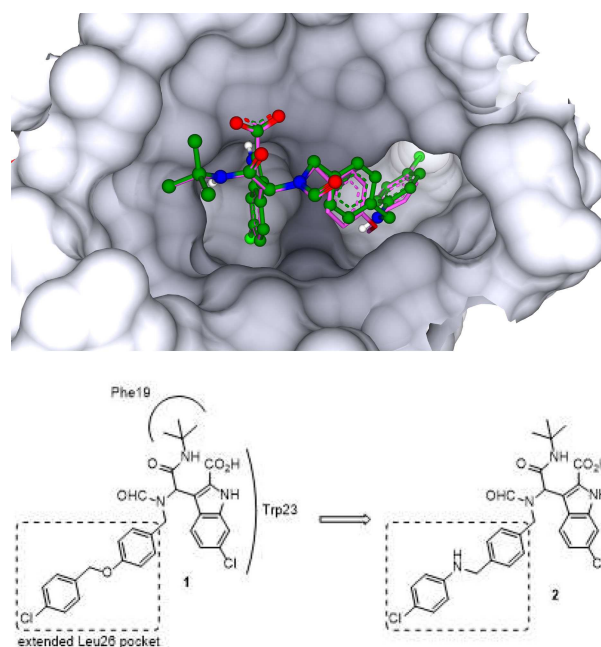


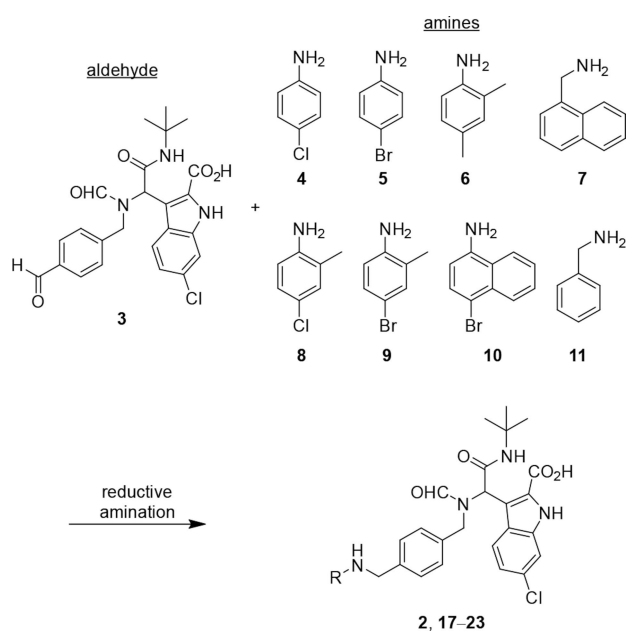
Figure 2. (Top) X-ray crystal structure of MDM2 in complex with docked inhibitor 1 (pink), superimposed with designed inhibitor 2 (green) (PDB ID: 4MDN). Oxygen, nitrogen and chlorine atoms are shown in red, blue and light green, respectively. (Bottom) Design of inhibitor 2 as a product of reductive amination, based on the previously reported inhibitor 1.

optimal way by using the reductive amination reaction, we converted the 4-chlorobenzyl ether moiety into an amine, which can be assembled from the corresponding aldehyde **3** and amine **4** followed by *in situ* reduction (Scheme 1).

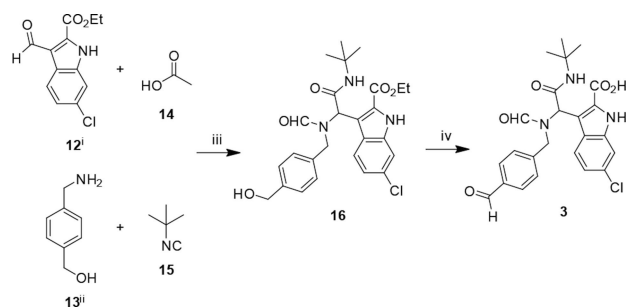
Following the design of the initial inhibitor, we generated a combinatorial library by using aldehyde **3** as a core scaffold and eight different amines (**4–11**) to explore and fill the extended Leu26 pocket in the best manner and give rise to a focused SAR (Scheme 1).

The use of KTGS to fill flexible pockets is unprecedented. To explore this binding pocket and possibly open-up the Leu26 pocket even further, we used a benzyl- and naphthyl-amine in the library in addition to the aromatic amines to extend the length of the linker between the core scaffold and the amines. A potential extension reaching deeper into the pocket would be an important finding for future drug development.

Having selected the building blocks from commercially available amines, we synthesized the core scaffold **3** as shown



**Scheme 1.** Selection of building blocks for the protein-templated reductive amination, which affords eight possible amine products.

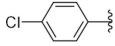
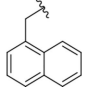
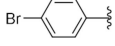
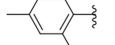
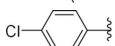
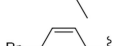
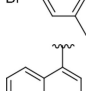
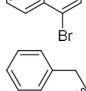


**Scheme 2.** Synthesis of aldehyde building block **3**. Conditions and reagents: i) three-step synthesis<sup>[41]</sup> ii) one-step synthesis<sup>[42]</sup> iii) MeOH, rt, 6 d, 63%; iv) a) DMP, CH<sub>2</sub>Cl<sub>2</sub>, rt, 3 h, b) 1 M LiOH, H<sub>2</sub>O-EtOH (1:1), rt, 18 h, 86%.

in Scheme 2. Literature protocols afforded compounds **12** and **13**, in three and one step(s), respectively.<sup>[41,42]</sup> A four-component Ugi reaction of aldehyde **12**, amine **13**, formic acid (**14**) and tert-butyl-isocyanide (**15**) furnished the corresponding Ugi product **16** in 63% yield. Oxidation of the alcohol and subsequent hydrolysis of the ester led to the final aldehyde **3** in 86% yield over two steps.

Biochemical evaluation of aldehyde building block **3** showed promising potency against MDM2 ( $K_i = 0.55 \pm 0.05 \mu\text{M}$ ). We envisioned that additional interactions in the flexible pocket would enhance compound potency. Therefore, we set up two experiments in parallel using the synthesized aldehyde building block and eight different commercially available amines (**4–11**), a protein-templated reaction and a blank reaction at pH=7.4 (100 mM phosphate buffer, 10% DMSO).

In both reactions, we applied standard building block and reducing agent concentrations of 100 and 200  $\mu\text{M}$ , respectively. One of the stringent requirements for KTGS is a substantial difference in reaction rate between the blank and the protein-templated reaction. As the imine formation between an aldehyde and an amine is fast, we used dilute conditions to prevent product formation in the reference reaction for a certain time.<sup>[43]</sup> As a result, less protein is required, an important consideration especially for precious proteins. By using a reducing agent in the reaction mixture from the beginning, formed imines would be “frozen” by reduction, leading to detectable amounts of products. Therefore, the two reactions were started by mixing all amines **4–11** (100  $\mu\text{M}$  each), aldehyde **3** (100  $\mu\text{M}$ ) and NaCNBH<sub>3</sub> (200  $\mu\text{M}$ ). To the protein-templated reaction, we added MDM2 (100  $\mu\text{M}$ ). Then, both reactions were carefully monitored using UPLC-MS analysis (wavelengths: 254 and 305 nm) for two days. After two days, signs of denaturation were observed in all MDM2-containing samples. We did not detect any trace of one of the reductive amination products, while a large amount of the starting materials were observed. Additionally, experiments in which MDM2 was replaced by bovine serum albumin (BSA), experiments without reducing agent and experiments in which the potent MDM2 inhibitor Nutlin-3 (100  $\mu\text{M}$ ,  $K_i = 36 \text{ nM}$ <sup>[44]</sup>) was added, showed identical results (Figures S10 and S11). In order to estimate how much of the product(s) should be formed for detection, we assessed the detection limit of the UPLC-MS. The UV-visible spectrum of **3** showed a clear absorption band around 305 nm (Figure S12). This wavelength has the benefit over 254 nm that there is a lot less background signal. Under identical conditions as the protein-templated reaction, the detection limit of aldehyde **3** was estimated to be  $< 2.6 \mu\text{M}$  and  $< 0.88 \mu\text{M}$  for 254 and 305 nm, respectively (Figures S13–15). In case only one reductive amination product were formed and taking into account the protein denaturation step with acetonitrile, this would correspond to as low as 1.8% conversion at 305 nm. Even if all eight amines reacted in a similar fashion, generating all possible products, this would require only 14% conversion of **3**. We believe that in order to claim a protein-templated reaction, we should be far above these numbers.

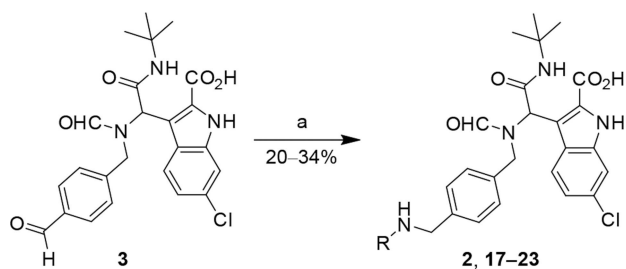
Inhibitor		$K_i$ [ $\mu\text{M}$ ] MDM2	$K_i$ [ $\mu\text{M}$ ] MDMX	Selectivity MDMX/MDM2
3	Aldehyde	$0.55 \pm 0.05$	$11.4 \pm 1.6$	$21 \pm 3.5$
2		$0.40 \pm 0.05$	$4.18 \pm 0.27$	$10 \pm 1.5$
17		$0.76 \pm 0.08$	$12.2 \pm 2.2$	$16 \pm 3.4$
18		$0.63 \pm 0.07$	$4.56 \pm 0.49$	$7.2 \pm 1.1$
19		$0.75 \pm 0.08$	$7.08 \pm 0.52$	$9.4 \pm 1.2$
20		$0.47 \pm 0.04$	$3.73 \pm 0.30$	$7.9 \pm 0.9$
21		$0.49 \pm 0.04$	$4.61 \pm 0.39$	$9.4 \pm 1.1$
22		$0.095 \pm 0.010$	$3.95 \pm 0.46$	$42 \pm 6.5$
23		$3.18 \pm 0.18$	$> 15$	$\geq 5$
	Nutlin-3 <sup>[44]</sup>	$0.036 \pm 0.009$	$9.38 \pm 0.35$	$261 \pm 66$

Experiments were performed in duplicate and values are reported as average  $\pm$  standard deviation. Note: at physiological pH, there is a difference in charge expected between the aniline-type products and benzylamine-type compounds 17 and 23.

In order to determine the potency of each product we synthesized all possible products (2 and 17–23, Table 1), starting from the core scaffold 3 by using a reductive amination protocol (Scheme 3).

We evaluated the inhibitory potency of compounds 2 and 17–23 by using the fluorescence polarization assay, as previously described.<sup>[45]</sup> MDMX is another p53 binding protein and shows significant homology with MDM2. In order to investigate if the compounds selectively inhibit one of the proteins, we tested all compounds against MDM2 and MDMX (Table 1).

As can be seen from Table 1, the majority of the compounds (2 and 17–21,  $K_i=0.40$ – $0.76 \mu\text{M}$ ) show an activity against MDM2 in the same range as aldehyde 3 ( $K_i=0.55 \pm 0.05 \mu\text{M}$ ) and parent compound 1 ( $K_i=0.60 \mu\text{M}$ ).<sup>[27]</sup> Amine 23 ( $K_i=3.18 \pm 0.18 \mu\text{M}$ ) is almost six-fold less potent than aldehyde 3.



Scheme 3. Synthesis of the inhibitors 2 and 17–23. (a) Conditions and reagents: amines 4–11, pyrrolidine, 4 Å MS,  $\text{Na}(\text{CH}_3\text{CO}_2)_3\text{BH}$ , dry  $\text{CH}_2\text{Cl}_2$ , rt, 18 h.

Interestingly, 18 ( $K_i=0.63 \pm 0.07 \mu\text{M}$ ) is three times more potent than its regioisomer in which the  $\text{CH}_2\text{-NH}$  is reversed ( $K_i=1.9 \mu\text{M}$ ).<sup>[28]</sup> Surprisingly, compound 22 shows a  $K_i$  value of  $0.095 \pm 0.010 \mu\text{M}$ , which makes it by far the most potent inhibitor of this series. In fact, the compound is almost as potent against MDM2 as Nutlin-3 ( $K_i=0.036 \pm 0.009 \mu\text{M}$ <sup>[44]</sup>).

The inhibitory activities of the synthesized reductive amination products against MDMX are rather comparable ( $K_i=3.73$ – $7.08 \mu\text{M}$ ). Except for compound 17 which has a slightly higher  $K_i$  of  $12.2 \pm 2.1 \mu\text{M}$  and 23, which is not active against MDMX under the applied conditions. Aldehyde 3 ( $K_i=11.4 \pm 1.6 \mu\text{M}$ ) also has a reduced inhibitory activity against MDMX in comparison to MDM2. Most compounds have a preference for MDM2 by a factor 7–16. With a selectivity factor of 21, aldehyde 3 is slightly more selective for MDM2 than most of the amines. A remarkable exception is compound 22, which is over four times more selective for MDM2 than inhibitors 2 and 18–21 and two times more selective than aldehyde 3. Although the activity of 22 against MDM2 is close to the  $K_i$  value of Nutlin-3, it is around six times less selective.

There are several possible explanations as to why we did not find any of the reductive amination products in the protein-templated experiments. Very recently, Van der Veken and co-workers reported their efforts toward the application of the Groebke-Blackburn-Bienaymé three-component reaction in KTGS.<sup>[46]</sup> The imine formation under near-physiological conditions proved to be most challenging. Furthermore, although their final products were also very potent against the protein target, the target itself interfered with the attempted reaction,

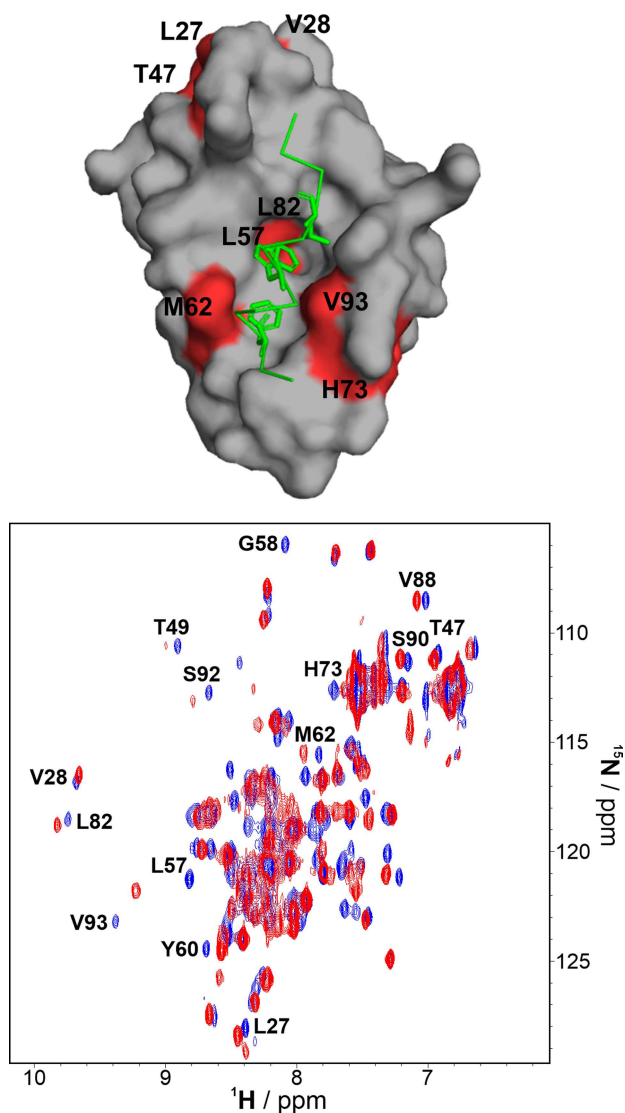


**Figure 3.** (Top) Chemical shift perturbations plotted onto the structure of the complex of MDM2 (grey) with p53 (green) (PDB ID: 1YCR<sup>[51]</sup>); residues which shift or disappear upon titration are labeled on the MDM2 surface (red). (Bottom) <sup>1</sup>H-<sup>15</sup>N HSQC NMR spectra: blue, reference spectrum of apo-MDM2; red, 1:5 (MDM2: inhibitor 17, over-titrated).

which could also be the case in our study. Additionally, it could be that the reducing agent does not reach the imine, which is therefore hydrolyzed upon analysis. Last, there are clear differences in rigidity and hydrogen-bond donor/acceptor profiles between the imines and the amines. It can well be that the aldehyde and reductive amination products show activity against MDM2, but that the imines cannot be formed or do not fit in the active site. We performed crystallization studies to confirm the binding mode of the new inhibitors, but due to solubility problems we could not obtain any crystals.

To confirm the inhibitory activity of the compounds further, the uniformly <sup>15</sup>N-labeled MDM2 was titrated with an increasing concentration of compound 17, and <sup>1</sup>H-<sup>15</sup>N HSQC spectra were recorded after each new portion of the inhibitor was added. Instead of the most potent compound, 22, compound 17 was

used due to its better solubility. The method is based on monitoring changes in NMR chemical shifts in protein amide backbone resonances upon its interaction with a small molecule.<sup>[47–50]</sup> In the course of titration, shifts or disappearances of cross-peaks assigned to the amino acids of MDM2 affected by binding of 17 were observed, which corroborates the binding event (Figure 3).

## Conclusions

In conclusion, herein, we reported our efforts toward the first example of a reductive amination in KTGS applied to a PPI target. By using our target MDM2 *in situ*, we screened a library of compounds in one-pot, which did not reveal a clear hit over a course of two days. After synthesis of all library members, we found a very potent and rather selective inhibitor of MDM2 ( $K_i = 0.095 \pm 0.010 \mu\text{M}$ ). Although, the KTGS method can find application in the early stages of drug discovery, one should be careful in the use of imine-based chemistry. Particularly interesting scenarios for the use of KTGS in drug discovery are flexible protein pockets that are difficult to target by structure-based approaches.

## Experimental Section

Detailed descriptions of the synthetic and biological procedures are provided in the Supporting Information.

## Acknowledgements

Funding was granted to A.K.H.H. by the Netherlands Organization for Scientific Research (NWO-CW, VIDI grant 723.014.008) and by the Helmholtz-Association's Initiative and Networking Fund; to A.K.H.H. and A.D. by the COFUND ALERT (grant agreement No. 665250); to T.A.H. by Grant UMO-2014/12/W/NZ1/00457 from the National Science Centre, Poland; and to A.D. by the National Institute of Health (NIH) (2R01 GM097082-05), the European Lead Factory (IM) under grant agreement number 115489, the Qatar National Research Foundation (NPRP6-065-3-012). Moreover, funding was received through ITN "Accelerated early stage drug discovery" (AEGIS, grant agreement No 675555), Hartstichting (ESCAPE-HF, 2018B012) and KWF Kankerbestrijding grant (grant agreement No. 10504).

- [1] M. Jaegle, E. L. Wong, C. Tauber, E. Nawrotzky, C. Arkona, J. Rademann, *Angew. Chem. Int. Ed.* **2017**, *56*, 7358–7378; *Angew. Chem.* **2017**, *129*, 7464–7485.
- [2] D. Bosc, J. Jakhilal, B. Deprez, R. Deprez-Poulain, *Future Med. Chem.* **2016**, *8*, 381–404.
- [3] M. Y. Unver, R. M. Gierse, H. Ritchie, A. K. H. Hirsch, *J. Med. Chem.* **2018**, *61*, 9395–9409.
- [4] M. Mondal, A. K. H. Hirsch, *Chem. Soc. Rev.* **2015**, *44*, 2455–2488.
- [5] P. Frei, R. Hevey, B. Ernst, *Chem. Eur. J.* **2019**, *25*, 60–73.
- [6] R. Nguyen, I. Huc, *Angew. Chem. Int. Ed.* **2001**, *40*, 1774–1776; *Angew. Chem.* **2001**, *113*, 1824–1826.

- [7] T. Maki, A. Kawamura, N. Kato, J. Ohkanda, *Mol. BioSyst.* **2013**, *9*, 940–943.
- [8] T. Asaba, T. Suzuki, R. Ueda, H. Tsumoto, H. Nakagawa, N. Miyata, *J. Am. Chem. Soc.* **2009**, *131*, 6989–6996.
- [9] L. Weber, *Drug Discovery Today Technol.* **2004**, *1*, 261–267.
- [10] E. Oueis, F. Nachon, C. Sabot, P.-Y. Renard, *Chem. Commun.* **2014**, *50*, 2043–2045.
- [11] S. S. Kulkarni, X. Hu, K. Doi, H.-G. Wang, R. Manetsch, *ACS Chem. Biol.* **2011**, *6*, 724–732.
- [12] S. E. Greasley, T. H. Marsilje, H. Cai, S. Baker, S. J. Benkovic, D. L. Boger, I. A. Wilson, *Biochemistry* **2001**, *40*, 13538–13547.
- [13] J. Inglese, S. J. Benkovic, *Tetrahedron* **1991**, *47*, 2351–2364.
- [14] W. G. Lewis, L. G. Green, F. Grynszpan, Z. Radić, P. R. Carlier, P. Taylor, M. G. Finn, K. B. Sharpless, *Angew. Chem. Int. Ed.* **2002**, *41*, 1053–1057; *Angew. Chem.* **2002**, *114*, 1095–1099.
- [15] R. Manetsch, A. Krasinski, Z. Radić, J. Raushel, P. Taylor, K. B. Sharpless, H. C. Kolb, *J. Am. Chem. Soc.* **2004**, *126*, 12809–12818.
- [16] A. Krasinski, Z. Radić, R. Manetsch, J. Raushel, P. Taylor, K. B. Sharpless, H. C. Kolb, *J. Am. Chem. Soc.* **2005**, *127*, 6686–6692.
- [17] X. Hu, J. Sun, H.-G. Wang, R. Manetsch, *J. Am. Chem. Soc.* **2008**, *130*, 13820–13821.
- [18] M. Gelin, G. Poncet-Montange, L. Assairi, L. Morellato, V. Huteau, L. Dugué, O. Dussurget, S. Pochet, G. Labesse, *Structure* **2012**, *20*, 1107–1117.
- [19] J. F. A. Chase, P. K. Tubbs, *Biochem. J.* **1969**, *111*, 225–235.
- [20] A. Dömling, *Curr. Opin. Chem. Biol.* **2008**, *12*, 281–291.
- [21] L. T. Vassilev, B. T. Vu, B. Craves, D. Carvajal, F. Podlaski, Z. Filipovic, N. Kong, U. Kammlott, C. Lukacs, C. Klein, *Science* **2004**, *303*, 844–848.
- [22] C. J. Brown, S. Lain, C. S. Verma, A. R. Fersht, D. P. Lane, *Nat. Rev. Cancer* **2009**, *9*, 862–873.
- [23] G. M. Popowicz, A. Dömling, T. A. Holak, *Angew. Chem. Int. Ed.* **2011**, *50*, 2680–2688; *Angew. Chem.* **2011**, *123*, 2732–2741.
- [24] Y. Zhao, A. Aguilar, D. Bernard, S. Wang, *J. Med. Chem.* **2015**, *58*, 1038–1052.
- [25] K. Khoury, G. M. Popowicz, T. A. Holak, A. Dömling, *MedChemComm* **2011**, *2*, 246–260.
- [26] D. Nguyen, W. Liao, S. X. Zeng, H. Lu, *Pharmacol. Ther.* **2017**, *178*, 92–108.
- [27] M. Bista, S. Wolf, K. Khoury, K. Kowalska, Y. Huang, E. Wrona, M. Arciniaga, G. M. Popowicz, T. A. Holak, A. Dömling, *Structure* **2013**, *21*, 2143–2151.
- [28] C. G. Neochoritis, J. Atmaj, A. Twarda-Clapa, E. Surmiak, L. Skalniak, L.-M. Köhler, D. Muszak, K. Kurpiewska, J. Kalinowska-Tłuścik, B. Beck, *Eur. J. Med. Chem.* **2019**, *182*, 111588.
- [29] I. Huc, J.-M. Lehn, *Proc. Natl. Acad. Sci. USA* **1997**, *94*, 2106–2110.
- [30] M. Hochgürtel, H. Kroth, D. Piecha, M. W. Hofmann, C. Nicolau, S. Krause, O. Schaaf, G. Sonnenmoser, A. V. Eliseev, *Proc. Natl. Acad. Sci. USA* **2002**, *99*, 3382–3387.
- [31] A. Valade, D. Urban, J.-M. Beau, *J. Comb. Chem.* **2007**, *9*, 1–4.
- [32] M. Hochgürtel, R. Biesinger, H. Kroth, D. Piecha, M. W. Hofmann, S. Krause, O. Schaaf, C. Nicolau, A. V. Eliseev, *J. Med. Chem.* **2003**, *46*, 356–358.
- [33] M. F. Schmidt, A. Isidro-Llobet, M. Lisurek, A. El-Dahshan, J. Tan, R. Hilgenfeld, J. Rademann, *Angew. Chem. Int. Ed.* **2008**, *47*, 3275–3278; *Angew. Chem.* **2008**, *120*, 3319–3323.
- [34] S. Zameo, B. Vauzeilles, J.-M. Beau, *Angew. Chem. Int. Ed.* **2005**, *44*, 965–969; *Angew. Chem.* **2005**, *117*, 987–991.
- [35] S. Zameo, B. Vauzeilles, J.-M. Beau, *Eur. J. Org. Chem.* **2006**, *2006*, 5441–5444.
- [36] G. Nasr, E. Petit, C. T. Supuran, J.-Y. Winum, M. Barboiu, *Bioorg. Med. Chem. Lett.* **2009**, *19*, 6014–6017.
- [37] G. Nasr, E. Petit, D. Vullo, J.-Y. Winum, C. T. Supuran, M. Barboiu, *J. Med. Chem.* **2009**, *52*, 4853–4859.
- [38] Z. Fang, W. He, X. Li, Z. Li, B. Chen, P. Ouyang, K. Guo, *Bioorg. Med. Chem. Lett.* **2013**, *23*, 5174–5177.
- [39] A. Valade, D. Urban, J.-M. Beau, *ChemBioChem* **2006**, *7*, 1023–1027.
- [40] SeeSAR version 9.2, BioSolveIT GmbH, Sankt Augustin (Germany), **2019**.
- [41] G. M. Popowicz, A. Czarna, S. Wolf, K. Wang, W. Wang, A. Dömling, T. A. Holak, *Cell Cycle* **2010**, *9*, 1104–1111.
- [42] J. Zheng, Y. Li, Y. Sun, Y. Yang, Y. Ding, Y. Lin, W. Yang, *ACS Appl. Mater. Interfaces* **2015**, *7*, 7241–7250.
- [43] C. Godoy-Alcántar, A. K. Yatsimirsky, J.-M. Lehn, *J. Phys. Org. Chem.* **2005**, *18*, 979–985.
- [44] S. Shangary, D. Qin, D. McEachern, M. Liu, R. S. Miller, S. Qiu, Z. Nikolovska-Coleska, K. Ding, G. Wang, J. Chen, *Proc. Natl. Acad. Sci. USA* **2008**, *105*, 3933–3938.
- [45] A. Czarna, G. M. Popowicz, A. Pecak, S. Wolf, G. Dubin, T. A. Holak, *Cell Cycle* **2009**, *8*, 1176–1184.
- [46] R. Gladysz, J. Vrijdag, D. Van Rompaey, A.-M. Lambeir, K. Augustyns, H. De Winter, P. Van der Veken, *Chem. Eur. J.* **2019**, *25*, 12380–12393.
- [47] Y. Li, C. Kang, *Molecules* **2017**, *22*, 1399–1419.
- [48] R. Powers, *Expert Opin. Drug Discovery* **2009**, *4*, 1077–1098.
- [49] E. Barile, M. Pellecchia, *Chem. Rev.* **2014**, *114*, 4749–4763.
- [50] L. D'Silva, P. Ozdow, M. Krajewski, U. Rothweiler, M. Singh, T. A. Holak, *J. Am. Chem. Soc.* **2005**, *127*, 13220–13226.
- [51] P. H. Kussie, S. Gorina, V. Marechal, B. Elenbaas, J. Moreau, A. J. Levine, N. P. Pavletich, *Science* **1996**, *274*, 948–953.

---

 Manuscript received: October 14, 2019

Revised manuscript received: November 21, 2019

Accepted manuscript online: November 27, 2019

Version of record online: December 12, 2019